

Low Potential and Non-Enzymatic Hydrogen Peroxide Sensor Based on Copper Oxide Nanoparticle on Activated Pencil Graphite Electrode

Mohammad Ali Kamyabi* and Nasim Hajari

Department of Chemistry, Colleges of Science, University of Zanjan, 4537138791 Zanjan, Iran

An electrochemical sensor for H_2O_2 determination was prepared by electrodepositing copper oxide nanoparticles on the activated pencil graphite electrodes. At first, a study has been made of the optimum conditions for chemical activation of the pencil graphite electrodes (APGE) and then the activated pencil graphite electrode was modified with copper oxide nanoparticles (CuO/APGE) and used as a non-enzymatic hydrogen peroxide sensor. The morphology of the modified electrode surface was investigated by scanning electron microscopy (SEM). Upon the addition of H_2O_2 , the modified electrode (CuO/APGE) exhibits significant oxidation of H_2O_2 with starting potential around +0.05 V (vs. Ag/AgCl) which dramatically decreases the overpotential of H_2O_2 oxidation. Under the optimal experiment conditions, the electrocatalytic response current of this sensor was proportional to the H_2O_2 concentration in the range of 5.0×10^{-6} to 1.6×10^{-3} mol L⁻¹ with a detection limit down to 0.21 μ mol L⁻¹ (signal/noise = 3). The sensitivity was calculated to be 4.75 μ AL mmol⁻¹. The electrochemical active surface area and the catalytic rate constant of hydrogen peroxide electro-oxidation were calculated. The H_2O_2 sensor exhibited a low detection limit, a good signal reproducibility (relative standard deviation (RSD), n = 4) 2.36% and the accurate measurements in milk as the real sample.

Keywords: pencil graphite electrode, non-enzymatic hydrogen peroxide sensor, electrocatalysis, CuO nanoparticle

Introduction

Hydrogen peroxide is an important chemical because it has attractive features like anti-bacterial property, decolorizing and oxidizing agent.¹ Widespread application in biology, as a product of oxidase-catalyzed reactions, industry and food make H_2O_2 as an attractive chemical to develop reliable and rapid detection methods for accurately monitoring of its concentration. Moreover, outstanding application in fuel cells as a carbon-free energy carrier and a strong oxidant in direct peroxide-peroxide fuel cell was recently developed.²

Various detection methods for hydrogen peroxide determination have been developed.³⁻⁵ Among them, the electrochemical method is preferable for its simplicity, high sensitivity and low detection limit. Considering the high catalytic activity and selectivity of enzymes for certain reactions, various enzymatic electrochemical biosensors have been constructed for the detection of hydrogen peroxide with excellent sensitivity, high selectivity and

rapid response,⁶ but the sensitivity of these sensors can be easily affected by temperature, pH value, humidity and toxic chemicals. Fabricated enzymatic sensors suffered greatly from the chief drawback of poor instability due to the intrinsic nature of enzymes. To solve this problem, the non-enzymatic sensors based on the direct oxidation of hydrogen peroxide have been explored for practical applications.⁷ Due to good reproducibility, low cost, fast response, high sensitivity, low detection limit, and high stability in aggressive environment, non-enzymatic amperometric sensors for direct determination of hydrogen peroxide have attracted considerable attention.⁸ At the opposite, one of the key problems in determination of non-enzymatic hydrogen peroxide is its high overpotential on the ordinary electrodes. Thus, the exploitation of new electrocatalyst with low overpotential has been intensively investigated during the past several decades.

Electrochemically active nanomaterials consisting of platinum,⁹ gold¹⁰ and carbon nanotubes¹¹⁻¹³ have been extensively studied for the electrochemical sensors, because they have large surface-to-volume ratio and increased catalytic activities. Of these, CuO nanomaterials are one of

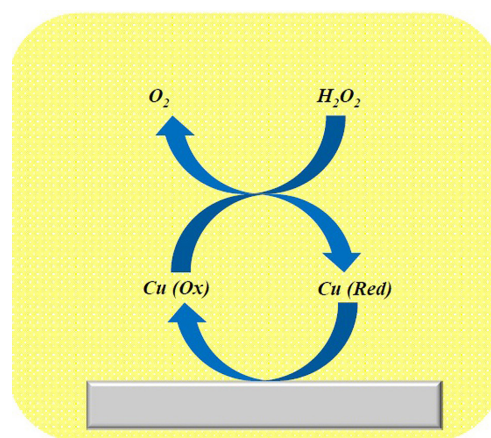
*e-mail: makamyabi@gmail.com

the promising candidates for the active electrode material due to their distinctive properties such as high stability and good electrical properties. Different synthetic methods have been studied for the preparation of CuO nanoparticles with various morphologies, including nanowire, nanosheet, nanorod, and nanoflower.^{14,15} Although most of metallic Cu⁰ nanomaterials are not stable enough to be used for electroanalysis because they are easily oxidized in air or aqueous solution, chemically more stable CuO nanomaterials have been studied for various applications including electrochemical H₂O₂ sensors.¹¹ The interesting occurrence of the growth of CuO nanowires during the *in situ* oxidation of copper in air has been reported intensively.¹⁶ Although this method can be categorized as a low cost method, it requires high temperature, high pressure, complex additives and long reaction time.¹⁷

The development of low-cost and sensitive electrodes for various electroanalytical applications is interested. The pencil graphite is easily accessible and useful material to prepare the modified electrode. The attractive property of a pencil graphite electrode (PGE) is its higher level of porosity compared to the glassy carbon electrode. Indeed, better intrinsic characteristics of the pencil graphite are attributed to its composite, consisting of graphite, polymeric binder and other additives (like clays).¹⁸ Indeed, the electron transfer properties of carbon electrodes can be improved by some types of pretreatment, which can be called the electrode "activation". The term "activation" has been used frequently to describe procedures for increasing the reactivity of carbon electrodes, often for the purpose of detecting a specific analyte. "Activation" can be involved in more than one mechanism in terms of its effects on the electrode surface.¹⁹ Many "activation" procedures are in fact cleaning steps and used to remove surface layers resulting from handling or impure materials used for polishing. Frequently, electrochemical oxidation or reduction in various media has long been used to "activate" carbon electrodes. Şentürk and co-authors²⁰ applied a potential of +1.4 V vs. Ag/AgCl for 60 s on the PGE surface in the selected supporting electrolyte without stirring to obtain a more sensitive and stable analytical signal. In another work, Özcan²¹ used synergic effect of chemical and electrochemical activation to activate the PGE.

Here, a new chemical activation method for the pencil graphite electrode was presented. Indeed, the PGE was chemically activated by stirring in an ethanolic HCl, which has been selected through an optimization method. Then, porous surface of the PGE was decorated with CuO nanocubes to promote electron transfer rate. This means that at the first step, the surface of the PGE was activated by the solution of ethanolic HCl 0.1 mol L⁻¹ to reach the activated PGE (APGE)

and then CuO nanoparticles were electrodeposited on the surface of APGE to fabricate CuO/APGE. The effect of the surface modification on the hydrogen peroxide oxidation was assessed by cyclic voltammetry (CV) and differential pulse voltammetry (DPV). The proposed modified electrode exhibited excellent catalytic activity, dramatic decrease in overpotential and high stability for hydrogen peroxide determination. Indeed, the fast chemical reaction between H₂O₂ and CuO converts Cu^{II} to Cu^I and H₂O₂ to O₂. As soon as Cu^I is produced, it is electro-oxidized back to Cu^{II} at the electrode surface and CuO continues the catalytic cycles (Scheme 1). The sensor was successfully used for the determination of hydrogen peroxide in milk samples using differential pulse voltammetric method.



Scheme 1. The schematic of the catalytic mechanism for the H₂O₂ oxidation by CuO nanomaterials.

Experimental

Reagents and apparatus

Hydrogen peroxide, ethanol, hydrochloric acid, copper sulfate, sodium sulfate, sodium hydroxide and phosphoric acid were purchased from Merck (Darmstadt, Germany). Double distilled water was used for the preparation of all solutions.

The pencil graphites were purchased as pencil lead from Rotring Co. Ltd. (Germany, R 505210N of type H). The diameter of all the pencil leads were 2.0 mm. All electrochemical experiments were performed using a micro Autolab potentiostat/galvanostat 101. The utilized three-electrode system was composed of modified APGE as the working electrode, Pt wire as a counter electrode and the potentials were measured *versus* Ag/AgCl (KCl 3 mol L⁻¹) reference electrode. Scanning electron micrograph (SEM) of the PGE, APGE and the modified electrode were performed by using TESCAN/Vega3. Electrochemical impedance spectroscopy (EIS) measurements were

performed by a Zahner Ennium potentiostat/galvanostat equipped with Thales USB software.

Preparation of the working electrode

The body of the pencil lead was tightly coated with a teflon band and the surface of the pencil lead was polished on a sandy paper and weighing paper to a smoothed finish before each use then rinsed with distilled water. Electrical contact with the lead was achieved by bonding a metallic contact to the working electrode. The pencil lead was fixed vertically and immersed in the solution in which the contact was only achieved via the cross section of the lead.

Chemical pretreatment of the PGE

At the first step, the chemical pretreatment of the surface of polished PGEs was carried out by 15 minutes stirring in ethanolic hydrochloric acid 0.1 mol L^{-1} to fabricate APGE. Ethanolic hydrochloric acid was selected as supporting electrolyte for the chemical activation and comparison with other electrolytes or the anodizing method. Then Cu/APGE was achieved by Cu electrochemical deposition method on the APGE surface by maintaining the potential at $-0.60 \text{ V vs. Ag/AgCl}$ for 240 s in $0.1 \text{ mol L}^{-1} \text{ Na}_2\text{SO}_4$ solution containing $0.02 \text{ mol L}^{-1} \text{ CuSO}_4$. After washing with water, the Cu/APGE was immersed in $0.1 \text{ mol L}^{-1} \text{ NaOH}$ and repeatedly scanned under the potential range from -0.40 to $+0.90 \text{ V}$ at scan rate of 0.1 V s^{-1} for 25 cycles. Deposition potential, deposition time, number of scans in NaOH were optimized by the final response to hydrogen peroxide in $0.1 \text{ mol L}^{-1} \text{ NaOH}$ as supporting electrolyte. During repetitive cyclic potential scanning in the alkaline solution of $0.1 \text{ mol L}^{-1} \text{ NaOH}$, CuO nanocubes were formed on the APGE. The repetitive cyclic voltammograms for the electrochemical deposition of CuO nanocubes on the APGE in $0.1 \text{ mol L}^{-1} \text{ NaOH}$ are shown in the Supplementary Information (Figure S1). The anodic peak can be attributed to the oxidation of Cu_2O and CuOH to CuO , while the cathodic peak can be attributed to the reduction of CuO into Cu_2O . During the cyclic potential scanning, all redox peak currents decreased, suggesting that CuO were formed during the CVs. The mechanism of oxidation in NaOH media is shown below:^{22,23}



Finally, the electrode was rinsed with water. The prepared modified electrode was named as CuO/APGE.

Results and Discussion

Selection of supporting electrolyte for activation of the PGE

To select the best electrolyte for activation of the PGE, $\text{K}_3\text{Fe}(\text{CN})_6$ was used as a known electrochemical probe. The peak currents and the separation of reduction and oxidation peaks potential were investigated as a monitoring factor.^{19,24,25} The oxidation peak current of the voltammetric responses of the APGE in different solution divided on the oxidation peak current of the unmodified PGE was given as an enhancement factor (equation 4). Also, the peak to peak separation was studied to investigate the reversibility of the modified electrodes. Figure 1 shows that a binary mixture of ethanol HCl 0.1 mol L^{-1} is a genuine nice enhancement factor. In consistence with enhancement factor, peak to peak separation has the least value in a binary mixture of ethanol HCl 0.1 mol L^{-1} (Figure 1). Although using an anodizing step can improve the response slightly, this step was ignored because stirring in ethanolic HCl achieves a higher efficiency. The HCl concentration in ethanol was also optimized (data not shown). The concentration of 0.1 mol L^{-1} was chosen as the optimum value for HCl in the subsequent experiments.

$$\text{Enhancement factor} = \frac{\text{Fe}(\text{CN})_6^{3-} \text{ oxidation current on modified PGE}}{\text{Fe}(\text{CN})_6^{3-} \text{ oxidation current on bare PGE}} \quad (4)$$

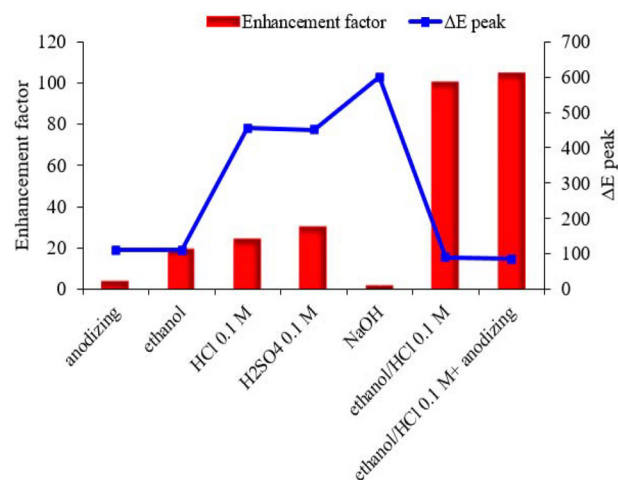


Figure 1. Comparison study of enhancement factor between different methods for activating PGE. The enhancement factor and peak to peak separation of 3.0 mmol L^{-1} ferrocyanide in $\text{KCl } 0.1 \text{ mol L}^{-1}$ on the APGE, in the presence of different solutions for 15 min, stirring rate: 250 rpm.

The actual mechanism of carbon electrode “activation” is still open to question; obviously, activation of pencil graphite surface is possible but the influence of the inert material, the pasting liquid in carbon paste electrodes,

for example, must be taken into account.^{26,27} We believe, however, that it is possible to stress the influence of the inert material too much and to de-emphasize the role of the carbon surface when interpreting the observed changes caused by the activation.²⁵ In PGE, removal of the pasting liquid probably does make more “active” sites available.

The surface characterization of the CuO/APGE

The morphology of PGE, APGE and CuO/APGE was studied by scanning electron microscopy characterization. As can be seen, the untreated PGE showed smooth surface morphology (Figures 2a and 2b), whereas APGE demonstrated the porous structure (Figures 2c and 2d), indicating that the chemical treatment process increased the surface roughness. This may arise from the breaking of the graphite layers into smaller parts during the chemical treatment process and it can be concluded that the chemical treatment increased the surface roughness. The cubic copper oxide particles are clearly visible on the porous PGE surface (Figures 2e and 2f). The average diameter of the electrodeposited particles was about 100 nm.

Electrochemical impedance spectroscopy was used to investigate the charge transfer property of the $\text{Fe}(\text{CN})_6^{3-/4-}$ redox couple at the bare and the modified APGE. The Nyquist plot of the EIS includes a semicircular part at high frequencies which refers to the electron-transfer limited process and a linear part at low frequencies which refers to the diffusion limited process. The diameter of semicircular portion is equal to the charge transfer resistance (R_{ct}), which shows the kinetic of electron transfer of the redox probe at the electrode interface. Figure 3 demonstrates that the R_{ct} value dramatically decreased after ethanolic HCl treatment. As expected, carbon electrodes, often for the purpose of detecting a specific analyte, need some types of pretreatments. The R_{ct} value was changed significantly by deposition of CuO nanocubes on the APGE.

In consistence with EIS results, cyclic voltammogram of $\text{Fe}(\text{CN})_6^{3-/4-}$ before and after deposition of CuO was illustrated in Supplementary Information (Figure S2). As can be seen in Figure S2, $\text{Fe}(\text{CN})_6^{3-/4-}$ has a reversible behavior with the peak to peak separation of about 70 mV and i_a/i_c is equal to 1, on the surface of the CuO/APGE electrode.

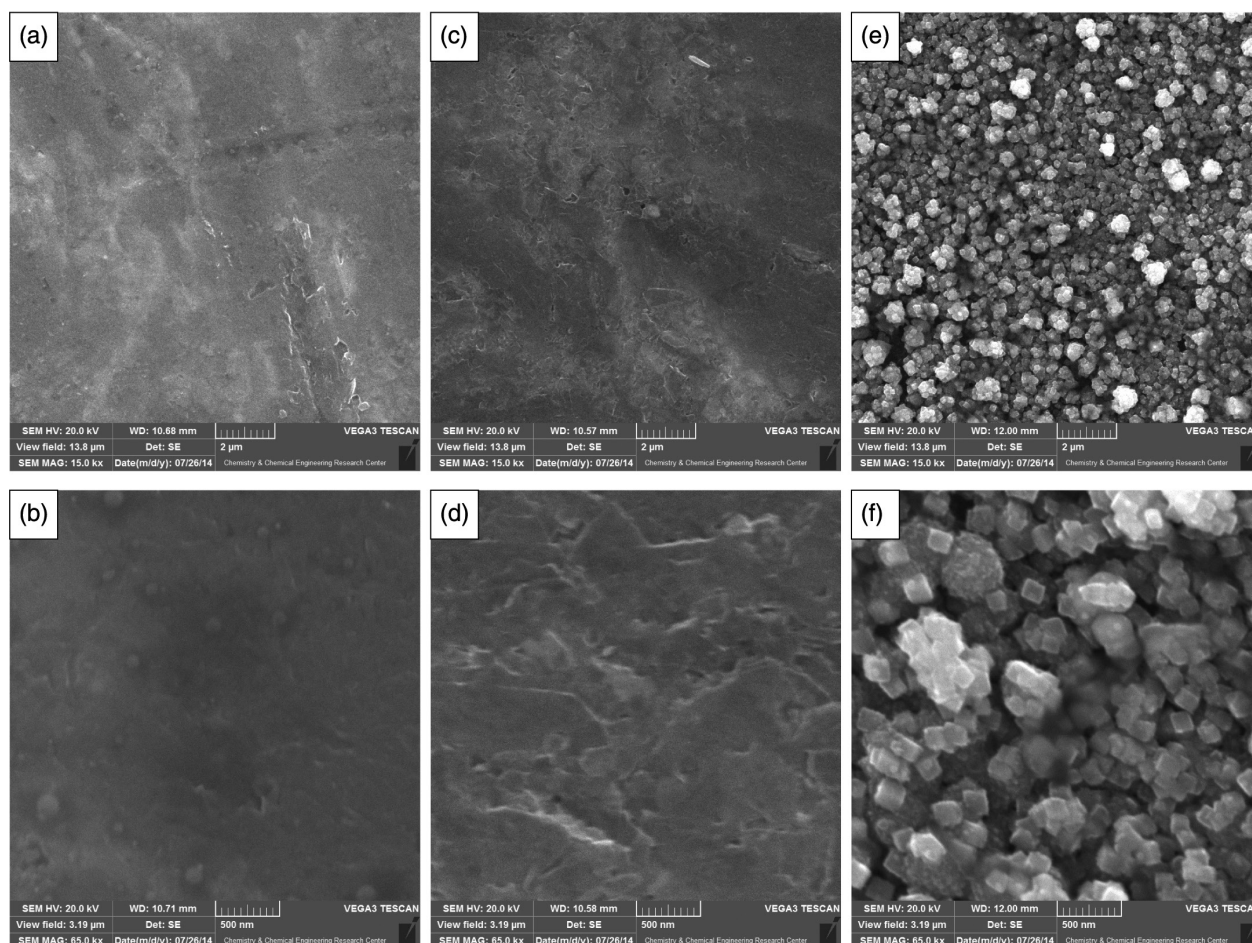


Figure 2. The SEM images of (a, b) PGE; (c, d) APGE and (e, f) CuO/APGE at 15.0 (a, c, e) and 65.0 (b, d, f) magnification.

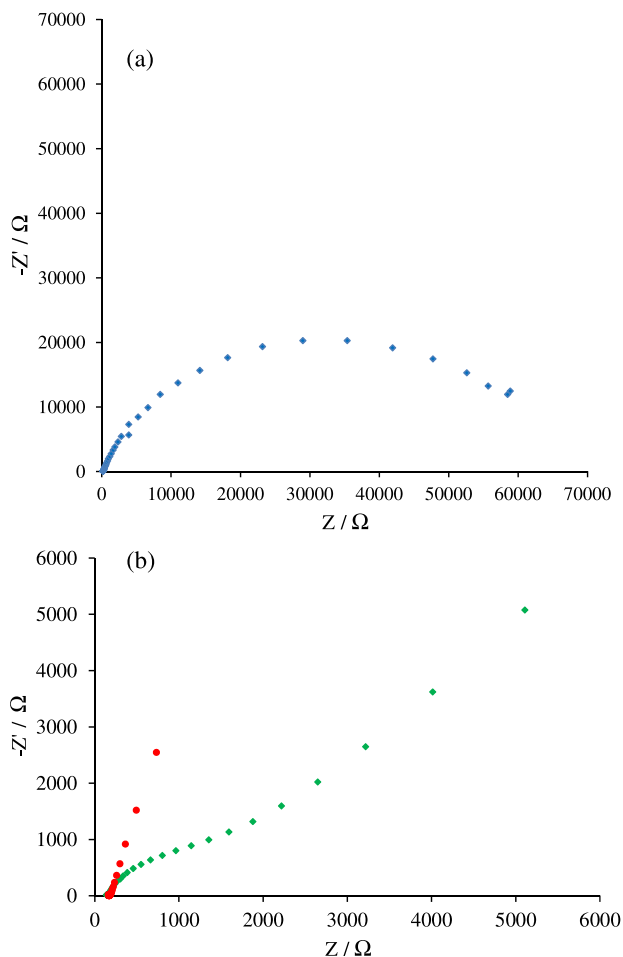


Figure 3. Nyquist plots of (a) PGE; (b) APGE (diamond) and CuO/APGE (circle) in a 0.1 mol L⁻¹ KCl containing 5.0 mmol L⁻¹ Fe(CN)₆^{3-/4-} at +0.2 V vs. Ag/AgCl, the frequency was scanned from 0.1 Hz to 100 kHz with the AC amplitude of 10 mV.

Figure 4a shows the cyclic voltammogram of CuO/APGE in 0.1 mol L⁻¹ NaOH with scan rate of 0.1 V s⁻¹. It includes two peaks during the anodic sweep which can be assigned to Cu⁰/Cu^I and Cu^I/Cu^{II} for the peaks I_a and II_a, respectively.^{28,29} During the cathodic sweep, two peaks also appeared, which can be assigned to the Cu^{II}/Cu^I and Cu^I/Cu⁰, respectively, while the redox peaks of Cu^{II}/Cu^{III} are not so clear.²⁶

To investigate the electrochemical behavior of the modified electrode, cyclic voltammograms of the CuO/APGE were recorded in the pH range of 3.0 to 13.0 (Figure 4b). The results show that increasing the solution pH the anodic and cathodic peak potentials of the electrode move to more negative potentials. The mean peaks potential ($E^{\circ'}$) at various pHs was calculated as the average value of the anodic and cathodic peaks potential of the voltammograms. As shown in Figure 4c (inset), increasing the pH solutions in the pH range of 3.0-8.0, $E^{\circ'}$ of CuO shift to negative values with the slope of about 29 mV pH⁻¹, which indicates that the redox process is pH dependent.

Electrocatalytic oxidation of H₂O₂

In this work, cyclic voltammetry was used to evaluate the electrocatalytic activity of the CuO/APGE towards H₂O₂ oxidation. As shown in Figures 5a and 5b, there were no electrochemical response to H₂O₂ on the surfaces of the bare PGE and also APGE in the applied potential window, while the CuO/APGE exhibits the oxidation response toward H₂O₂ oxidation (Figure 5c).

As illustrated in Figure 5d, by increasing the concentration of H₂O₂ at the CuO/APGE, the anodic peak current increased, which indicates good electrocatalytic activity of CuO/APGE towards H₂O₂ oxidation. Here, in the anodic pathway, Cu^I is oxidized electrochemically to Cu^{II} (i.e., Cu₂O + 2OH⁻ → 2CuO + H₂O + 2e⁻). In the presence of H₂O₂, according to standard redox potential of H₂O₂ to O₂ and CuO to Cu₂O in the alkaline media (Supplementary Information, Table S1), Cu^{II} chemically converts to Cu^I (i.e., 2CuO + H₂O₂ → Cu₂O + H₂O + O₂). As soon as Cu^{II} is reduced to Cu^I by H₂O₂, it is electro-oxidized back to Cu^{II} at the electrode surface.³⁰ Therefore, in the anodic scan, the local concentration of Cu^I at the electrode surface is increased in the presence of H₂O₂, thus the anodic current is increased. Increasing the anodic peak current depends on the H₂O₂ concentration. Since the above chemical reaction between H₂O₂ and CuO is fast, nano-copper oxide particles were suitable as mediators to shuttle electrons between H₂O₂ and working electrode.²³

For comparison, CuO was formed on the bare PGE and stabilized with cycling in NaOH. The CuO nanoparticles on the untreated PGE were not stable and a dramatic decrease was observed via cycling in the NaOH media. This result revealed the basic role of activated treatment on the PGE. This is due to the fact that APGE has a wide surface area and the copper nanoparticles could stand on these sites. H₂O₂ electrocatalytic oxidation mechanism at the CuO/APGE is indicated in Scheme 1. The CuO nanoparticles can oxidize the H₂O₂ to O₂ via the generation of Cu^I by the following reaction:²⁰

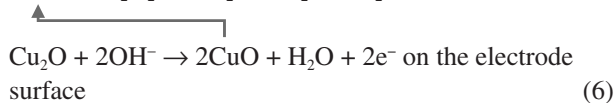
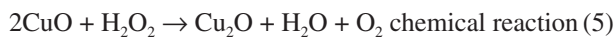


Figure 6a shows the cyclic voltammograms of 1.0 mmol L⁻¹ H₂O₂ in NaOH 0.1 mol L⁻¹ on the CuO/APGE at different scan rates ranging from 10 to 500 mV s⁻¹. The peak currents are linearly proportional to the square root of scan rate in the range of 10-400 mV s⁻¹, indicating a diffusion controlled electron process occurred for H₂O₂

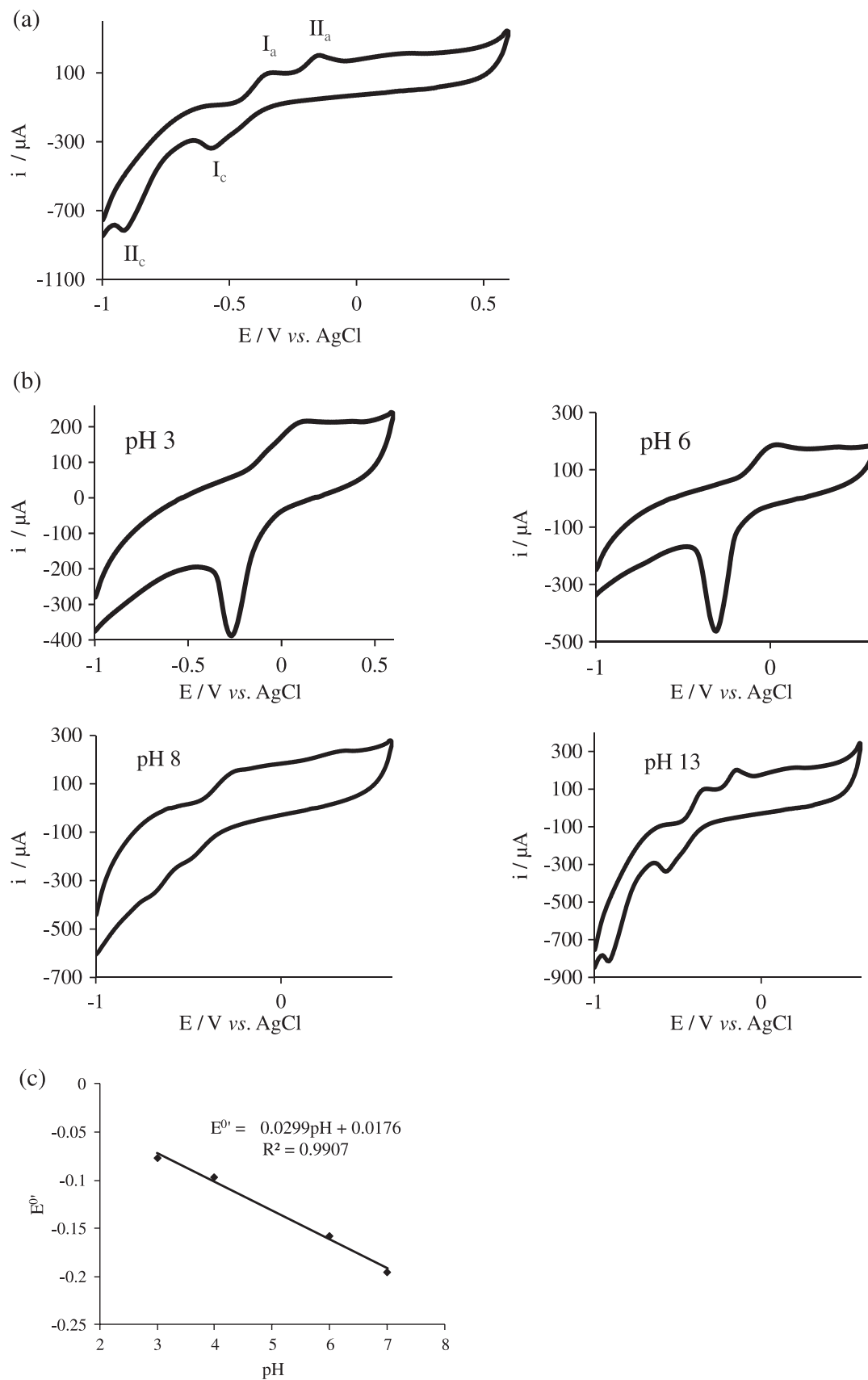


Figure 4. (a) Cyclic voltammogram of CuO/APGE in the 0.1 mol L⁻¹ NaOH with scan rate of 100 mV s⁻¹; (b) effect of pH on the CuO/APGE, scan rate: 100 mV s⁻¹; (c) the inset shows the dependence of E^0 vs. pH in the pH range of 3.0-8.0.

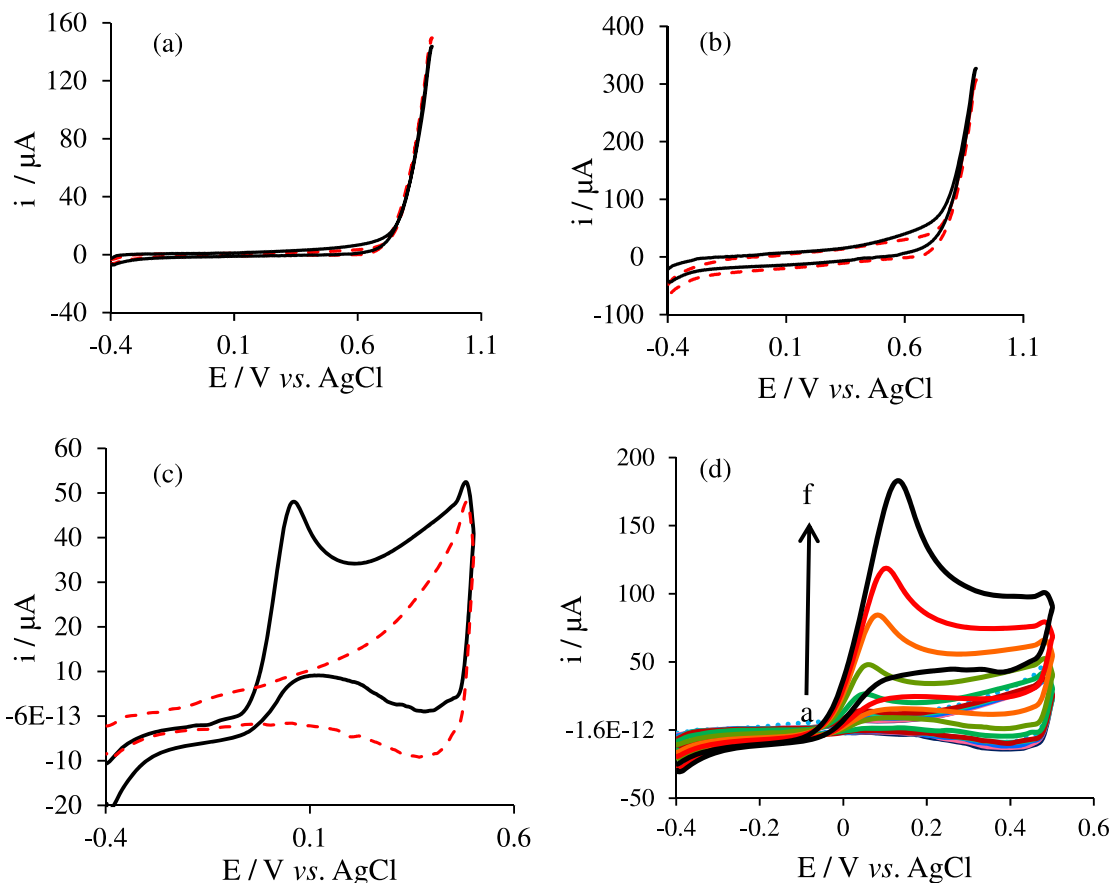


Figure 5. Cyclic voltammogram of (a) PGE; (b) APGE and (c) APGE/CuO in $0.1 \text{ mol L}^{-1} \text{ NaOH}$, in presence (black solid line) and absence (red dashed line) of $6.0 \text{ mmol L}^{-1} \text{ H}_2\text{O}_2$, scan rate 0.1 V s^{-1} ; (d) cyclic voltammograms of CuO/APGE with addition of H_2O_2 from 0.11 to 29.9 mmol L^{-1} in $0.1 \text{ mol L}^{-1} \text{ NaOH}$, scan rate 0.1 V s^{-1} .

determination, which is the perfect manner for quantitative determinations (Figure 6b). Moreover, the oxidation potential was almost the same at scan rates below 50 mV s^{-1} , suggesting facile charge transfer kinetics over this range of sweep rates. On the other hand, it was found that at scan rates above 50 mV s^{-1} , the oxidation peak potential were increased with scan rate increasing. The values of oxidation potential are proportionate to the logarithm of the current (data not shown). Based on the Tafel theory, the transfer coefficient (α) can be estimated by measuring the variation of peak potential with current.³¹ The transfer coefficient at scan rate 10 mV s^{-1} in the presence of $1.0 \text{ mmol L}^{-1} \text{ H}_2\text{O}_2$ was obtained as 0.53.

The chronoamperometry as well as other electrochemical methods was employed for investigation of electrode processes at the modified electrodes. Figure 7a illustrates the chronoamperometric measurements of the system at the CuO/APGE. This figure represents the current-time curves obtained by setting the working electrode potential at $200 \text{ mV vs. Ag/AgCl}$ in the absence and presence of hydrogen peroxide. Figure 7b shows the experimental plot of i vs. $t^{1/2}$. The slope of the resulting straight line was then

plotted against hydrogen peroxide concentration. From the slope and using the Cottrell equation,³² the value of diffusion coefficient was found to be $9.55 \times 10^{-6} \text{ cm}^2 \text{ s}^{-1}$.

$$I = nFAD^{1/2}C_0 \pi^{-1/2}t^{-1/2} \quad (7)$$

where I , n , F , A , D , C_0 , and t refer to the current, number of electrons, Faraday constant, area of the working electrode, diffusion coefficient, initial mole concentration of Cu, and time, respectively.

According to the method described in, chronoamperometric data can also be employed to evaluate the catalytic rate constant of the chemical reaction between the hydrogen peroxide and the active site of the CuO/APGE according to the following equation:³³

$$i_c/i_l = \gamma^{1/2}[\pi^{1/2} \text{erf}(\gamma^{1/2}) + \exp(-\gamma)/\gamma^{1/2}] \quad (8)$$

where i_c is the catalytic current of the CuO/APGE in the presence of hydrogen peroxide, i_l is the limiting current in the absence of hydrogen peroxide and $\gamma = kC_0t$, where C_0 is the bulk concentration of hydrogen peroxide (mol L^{-1}), k is

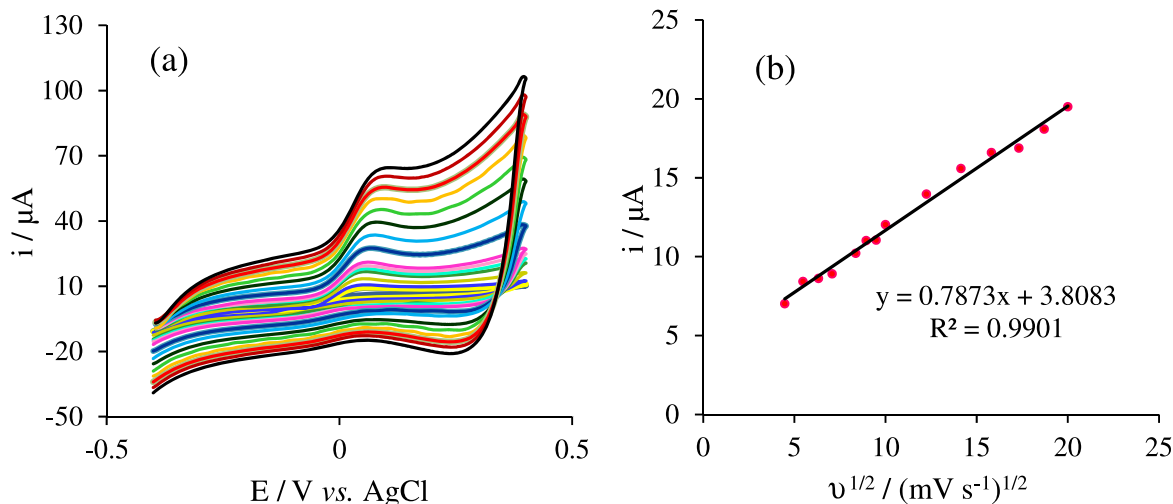


Figure 6. (a) Cyclic voltammograms of CuO/APGE NaOH 0.1 mol L⁻¹ solution containing 1.0 mmol L⁻¹ H₂O₂ at the scan rates from 10 to 500 mV s⁻¹; (b) plot of variations of peak currents (*i_p*) versus $v^{1/2}$.

the catalytic rate constant ($\text{cm}^3 \text{mol}^{-1} \text{s}^{-1}$) and t is the time elapsed (s), and $\text{erf}(\gamma^{1/2})$ is the argument of error function. In treatments, it is assumed that hydrogen peroxide is present in large excess rather than Cu nanocubes, in addition where γ exceeds 2, the error function is almost equal to 1 and the above equation can be considered as follows:

$$i_c/i_1 = \gamma^{1/2} \pi^{1/2} = \pi^{1/2} (kC_0 t)^{1/2} \quad (9)$$

Based on the slope of the i_c/i_1 vs. $t^{1/2}$ plot (Figure 7c), the mean value of k was found to be $33.47 \text{ cm}^3 \text{mol}^{-1} \text{s}^{-1}$ in the

$3.84 \text{ mmol L}^{-1} \text{H}_2\text{O}_2$ solution. This value for the electron transfer rate constant is comparable with $41.9 \text{ cm}^3 \text{mol}^{-1} \text{s}^{-1}$ for Hb/PLE, the apparent heterogeneous electron transfer rate constant reported previously.³³

Differential pulse voltammetric determination of H₂O₂ at the CuO/APGE

Due to the more quantitative features of differential pulse voltammetry to cyclic voltammetry method, this electrochemical technique was employed to obtain the

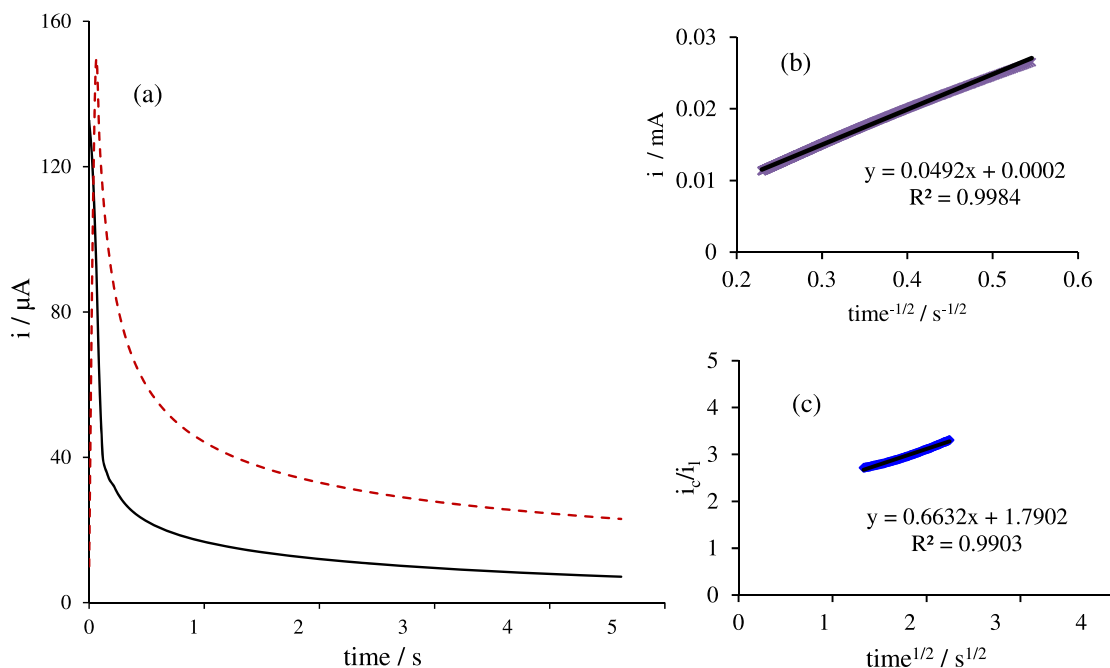


Figure 7. (a) Chronoamperograms of CuO/APGE in 0.1 mol L⁻¹ NaOH solution in absence (black solid line) and presence of 3.84 mmol L⁻¹ H₂O₂ (red dashed line), potential step was 0.2 V; (b) dependency of transient current on $t^{1/2}$ for following concentration of hydrogen peroxide; (c) dependence of (i_c/i_1) on $t^{1/2}$ derived from the data of chronoamperogram.

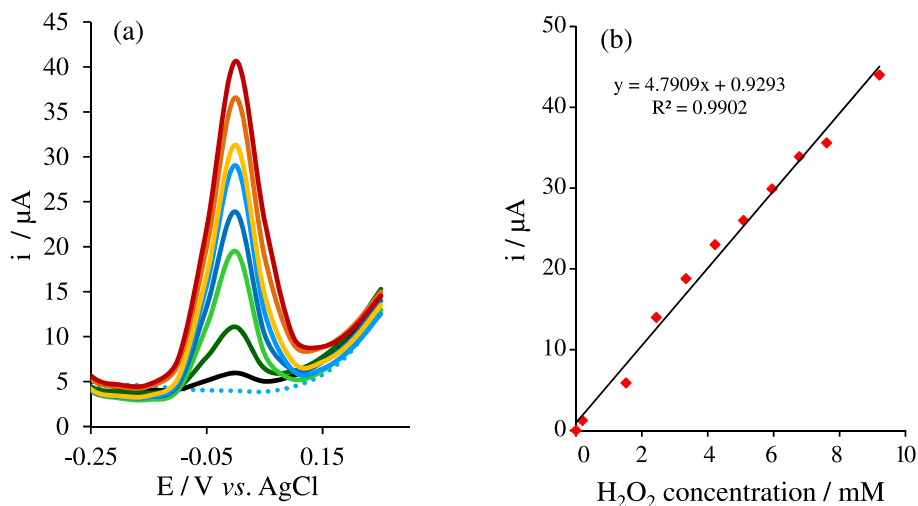


Figure 8. (a) DP voltammograms for hydrogen peroxide determination. The DPV parameters are $\alpha = 50$ mV, $\tau = 50$ ms, $v = 0.1$ V s $^{-1}$, and NaOH solution (0.1 mol L $^{-1}$); (b) calibration curve of concentration *versus* peak current of H₂O₂.

analytical figures. In order to obtain the calibration curve, the measurements were performed in 0.1 mol L $^{-1}$ NaOH solution with the hydrogen peroxide addition in the concentration range of 5.0×10^{-6} to 2.6×10^{-3} mol L $^{-1}$ (Figure 8).

The analytical curve is linear in the hydrogen peroxide concentration range from 5.0 μ mol L $^{-1}$ to 2.6 mmol L $^{-1}$ with a limit of detection (LOD) of 0.21 μ mol L $^{-1}$. LOD was calculated using the relationship $3s/b$, where s is the average of standard deviation of 4 measurements for the blank solution and b is the sensitivity calculated from the calibration curve slope (4.75 μ AL mmol $^{-1}$).

For comparison, the performances of the CuO/APGE and the other hydrogen peroxide sensors reported in literature were listed in Table 1. As can be seen in Table 1, an outstanding feature of the developed sensor is the significant decrease in overpotential for hydrogen

peroxide oxidation. Moreover, the presented sensor exhibits comparable analytical figures while it has low cost and easily preparation merits. Although some sensors have a wider linear range, their outstanding low determination potential is an attractive feature in the presented sensor.

Reproducibility and stability of the H₂O₂ sensor

Reproducibility and stability are attractive features for sensors. To establish the reproducibility, four modified electrodes were fabricated and their DP voltammetric responses towards 1.0 mmol L $^{-1}$ H₂O₂ were examined. The relative standard deviation (RSD, $n = 4$) was found to be 2.36%. The storage stability was investigated by recording DP voltammetric response of 1.0 mmol L $^{-1}$ H₂O₂ in 0.1 mol L $^{-1}$ NaOH, during 10 days. CuO/APGE retained 95% of its initial current response for hydrogen

Table 1. Analytical performances of different modified electrodes for H₂O₂ determination

Sensor	LDR / (mol L $^{-1}$)	DL / (μ mol L $^{-1}$)	Sensitivity / (μ AL mmol $^{-1}$)	Oxidation potential / V vs. Ag /AgCl	Reference
Nano-TiO ₂ and Pt/Ti foil	4×10^{-6} to 1.25×10^{-3}	4	0.85	0.3	34
Pt-implanted/boron-doped diamond electrode	1.0×10^{-7} to 1.0×10^{-5}	0.03	21.9	0.55	35
Copper on porous silicon (Cu/PSi)-CPE	5.0×10^{-4} to 3.78×10^{-3}	0.27	13.09	0.2	23
Carbon nanofiber/GC	1.80×10^{-4} to 2.62×10^{-3}	4	3.20	0.65	36
Carbon nanotube paste electrode	not reported	20	0.8	0.95	37
AuNPs/MWCNT/PANI	3.0×10^{-6} to 6.0×10^{-4}	0.3	3.3	0.8	38
Cu/GC	2.0×10^{-9} to 2.7×10^{-7}	0.0002	1.24×10^{-4}	0.2	23
MnO ₂ /OMC/GC	5×10^{-7} to 6×10^{-4}	0.07	806.8μ AL mmol $^{-1}$ cm $^{-2}$	0.45	39
CuO/APGE	5.0×10^{-6} to 1.6×10^{-3}	0.21	4.75	0.05	this work

PANI: polyaniline; MWCNTs: multiwalled carbon nanotubes; AuNPs: gold nanoparticles; CPE: carbon paste electrode; GC: glassy carbon; OMC: ordered mesoporous carbon; APGE: activated pencil graphite electrode.

peroxide over a 10 day period. These results indicate that this electrochemical sensor has a good stability and reproducibility, as required for the determination of H₂O₂.

Interference study and real sample analysis

The selectivity studies are challenging problems for enzyme-free H₂O₂ sensors in the presence of common interfering species, though the naturally coexisting interfering species are highly active at enzyme-free electrode systems.⁴⁰ The DP voltammetric response of the CuO/APGE to the consecutive addition of H₂O₂ (0.4 mmol L⁻¹) and potentially interfering species such as ascorbic acid, uric acid and glucose (0.4 mmol L⁻¹) in 0.1 mol L⁻¹ NaOH, were recorded. In practical conditions, glucose and uric acid did not disturb in the detection of hydrogen peroxide and ascorbic acid interference response is less than 3%. Indeed, the good selectivity can be attributed to dramatic decrease in electrocatalytic oxidation potential of hydrogen peroxide.

To demonstrate electrode suitability and potential application for sample analysis, the CuO/APGE was used for the determination of H₂O₂ in ultra-high-temperature (UHT) processed milk. Hydrogen peroxide in milk samples presents as a result of enzymatic activity and works as an anti-bacterial agent.⁴¹ While the amount of hydrogen peroxide in milk is lower than detection limit, the sample was spiked with various amounts of H₂O₂ and a recovery test was performed (Table 2). The recovery was about 97.5% by four replications suggesting that there was no interference from the complex matrix of milk.

Table 2. Results of determination of hydrogen peroxide in the milk samples

Detected amount	Spiked / (mmol L ⁻¹)	Found / (mmol L ⁻¹)	Recovery / %
–	1.0	0.98	98
–	3.0	2.91	97

Conclusions

In summary, a low potential electrochemical sensor was presented for hydrogen peroxide determination. A porous electrode with high surface area could be achieved by electrodeposition of CuO nanocubes on the APGE. The presented sensor is prepared in less than one hour with the lowest cost. The CuO-modified electrode displayed high electrocatalytic activity and fast response to hydrogen peroxide oxidation. This CuO/APGE electrochemical sensor has comparable analytical figures with other

electrochemical sensors. The relative standard deviation (RSD, n = 4) was 2.36%. These results indicate that this electrochemical sensor has a good reproducibility, as required for the determination of H₂O₂.

Supplementary Information

Supplementary information is available free of charge at <http://jbcs.org.br> as PDF file.

Acknowledgment

The authors express their gratitude to the University of Zanjan Research Council for support of this work.

References

- Lin, K.-C.; Yin, C.-Y.; Chen, S.-M.; *Sens. Actuators, B* **2011**, *157*, 202.
- Yang, F.; Cheng, K.; Xue, X.; Yin, J.; Wang, G.; Cao, D.; *Electrochim. Acta* **2013**, *107*, 194.
- Klassen, N. V.; Marchington, D.; McGowan, H. C.; *Anal. Chem.* **1994**, *66*, 2921.
- Sellers, R. M.; *Analyst* **1980**, *105*, 950.
- Paital, B.; *BioMed Res. Int.* **2014**, *2014*, ID 342958.
- Gao, Z.; Liu, J.; Chang, J.; Wu, D.; He, J.; Wang, K.; Xu, F.; Jiang, K.; *CrystEngComm* **2012**, *14*, 6639.
- Wu, H.-X.; Cao, W.-M.; Li, Y.; Liu, G.; Wen, Y.; Yang, H.-F.; Yang, S.-P.; *Electrochim. Acta* **2010**, *55*, 3734.
- Li, K.; Fan, G.; Yang, L.; Li, F.; *Sens. Actuators, B* **2014**, *199*, 175.
- Guo, S.; Wen, D.; Zhai, Y.; Dong, S.; Wang, E.; *ACS Nano* **2010**, *4*, 3959.
- Maduraiveeran, G.; Ramaraj, R.; *J. Electroanal. Chem.* **2007**, *608*, 52.
- Yang, N.; Chen, X.; Ren, T.; Zhang, P.; Yang, D.; *Sens. Actuators, B* **2015**, *207*, 690.
- Kamyabi, M. A.; Hajari, N.; Turner, A. P.; Tiwari, A.; *Talanta* **2013**, *116*, 801.
- Kamyabi, M. A.; Rahmanian, N.; *Anal. Methods* **2015**, *7*, 1339.
- Song, M.-J.; Hwang, S. W.; Whang, D.; *Talanta* **2010**, *80*, 1648.
- Prathap, M. A.; Kaur, B.; Srivastava, R.; *J. Colloid Interface Sci.* **2012**, *370*, 144.
- Li, A.; Song, H.; Wan, W.; Zhou, J.; Chen, X.; *Electrochim. Acta* **2014**, *132*, 42.
- Lu, L.; Huang, X.; *Microchim. Acta* **2011**, *175*, 151.
- McCreery, R. L.; *Advanced Carbon Electrode Materials for Molecular Electrochemistry*, vol. 17; Bard, A. J., ed.; Marcel Dekker: New York, 1990, p. 221.
- McCreery, R. L.; *Chem. Rev.* **2008**, *108*, 2646.

20. Yardım, Y.; Keskin, E.; Levent, A.; Özsöz, M.; Şentürk, Z.; *Talanta* **2010**, *80*, 1347.
21. Özcan, A.; *Electroanalysis* **2014**, *26*, 1631.
22. Yang, J.; Jiang, L.-C.; Zhang, W.-D.; Gunasekaran, S.; *Talanta* **2010**, *82*, 25.
23. Le, W.-Z.; Liu, Y.-Q.; *Sens. Actuators, B* **2009**, *141*, 147.
24. Lord Jr., S.; Rogers, L.; *Anal. Chem.* **1954**, *26*, 284.
25. Tavares, P. H. C. P.; Barbeira, P. J. S.; *J. Appl. Electrochem.* **2008**, *38*, 827.
26. Rice, M. E.; Galus, Z.; Adams, R. N.; *J. Electroanal. Chem. Interfacial Electrochem.* **1983**, *143*, 89.
27. Urbaniczky, C.; Lundström, K.; *J. Electroanal. Chem. Interfacial Electrochem.* **1984**, *176*, 169.
28. Zhang, Y.; Su, L.; Manuzzi, D.; de los Monteros, H. V. E.; Jia, W.; Huo, D.; Hou, C.; Lei, Y.; *Biosens. Bioelectron.* **2012**, *31*, 426.
29. Ensafi, A. A.; Abarghoui, M. M.; Rezaei, B.; *Sens. Actuators, B* **2014**, *196*, 398.
30. Yang, Y. J.; Zi, J.; Li, W.; *Electrochim. Acta* **2014**, *115*, 126.
31. Bard, A. J.; Faulkner, R. W. In *Electrochemical Methods, Fundamentals and Applications*; Wiley: New York, 2004, p. 23.
32. Jafarian, M.; Haghghatbin, M.; Gobal, F.; Mahjani, M.; Rayati, S.; *J. Electroanal. Chem.* **2011**, *663*, 14.
33. Majidi, M. R.; Pournaghi-Azar, M. H.; Saadatirad, A.; Alipour, E.; *Food Anal. Methods* **2015**, *8*, 1067.
34. Cui, X.; Li, Z.; Yang, Y.; Zhang, W.; Wang, Q.; *Electroanalysis* **2008**, *20*, 970.
35. Ivandini, T. A.; Sato, R.; Makide, Y.; Fujishima, A.; Einaga, Y.; *Diamond Relat. Mater.* **2005**, *14*, 2133.
36. Li, Z.; Cui, X.; Zheng, J.; Wang, Q.; Lin, Y.; *Anal. Chim. Acta* **2007**, *597*, 238.
37. Valentini, F.; Amine, A.; Orlanducci, S.; Terranova, M. L.; Palleschi, G.; *Anal. Chem.* **2003**, *75*, 5413.
38. Narang, J.; Chauhan, N.; Pundir, C.; *Analyst* **2011**, *136*, 4460.
39. Luo, L.; Li, F.; Zhu, L.; Zhang, Z.; Ding, Y.; Deng, D.; *Electrochim. Acta* **2012**, *77*, 179.
40. Karuppiyah, C.; Palanisamy, S.; Chen, S.-M.; *Electrocatalysis* **2014**, *5*, 177.
41. Harrison, R.; *Int. Dairy J.* **2006**, *16*, 546.

Submitted: February 23, 2016

Published online: August 12, 2016